SHORT THESIS FOR THE DEGREE OF DOCTOR OF PHILOSOPHY (PhD)

Perspectives of Imaging Cytometry and its implication in High content screening

by Minh Doan, MD

Supervisor: Zsolt Bacsó, MD, PhD

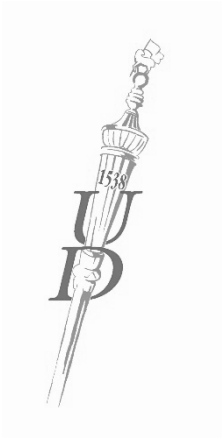

UNIVERSITY OF DEBRECEN

DOCTORAL SCHOOL OF MOLECULAR CELL AND IMMUNE BIOLOGY

DEBRECEN, 2015

Perspectives of imaging cytometry and its implication in High content screening

by Minh Doan, MD

Supervisor: Zsolt Bacsó, MD, PhD

Doctoral School of Molecular Cell and Immune Biology, University of Debrecen

Head of the **Examination Committee**:	Prof. László Virág, MD, PhD, DSc
Members of the Examination Committee:	Prof. János Magyar, MD, PhD, DSc
	László Homolya, PhD, DSc

The examination takes place at the Department of Medical Chemistry, Life Science Building, Faculty of Medicine, University of Debrecen at 10:30 AM, August 27, 2014.

Head of the **Defense Committee**:	Prof. László Virág, MD, PhD, DSc
Reviewers:	Máté Demény, MD, PhD
	James F. Eliason, PhD
Members of the Defense Committee:	Prof. János Magyar, MD, PhD, DSc
	Prof. Miklós Nyitrai, PhD, DSc

The PhD Defense takes place at the Lecture Hall of Building A, Department of Internal Medicine, Faculty of Medicine, University of Debrecen at 13:00 PM, February 9, 2015.

1. Introduction

1.1 An overview of cytometry techniques

Knowledge regarding the complexity of a cell has grown tremendously over the last century. The infinite changes that can occur in an individual cell under different conditions represent a myriad of data for scientists to mine. Through the marvels of 21st century technology, cell biologists have witnessed major technological advances that have led to a steady development of cellular measurements.

The key concept in cytometry is to collect and evaluate physical and chemical characteristics of single cells, and at the same time taking into account statistical distribution of these parameters in cell populations. Based on this concept, fluorescence-based flow cytometry was developed and became a dominating method for objective cell measurement. Although flow cytometry could satisfy this requirement and is indeed a powerful multiparametric tool to reveal heterogeneity of cell populations, sampled cells should be in suspension, meaning that cultured adherent cells should be detached mechanically or enzymatically. These treatments can interfere with cellular parameters to be investigated. Due to the nature of operation, original flow cytometry system gives only one value in a channel for one flow-by cell; if there is a cellular change upon stimulus, flow cytometry cannot provide information about the time course of a response in a single cell. In addition, due to the lack of photographing ability, the intracellular pattern of a cell can hardly be studied.

Image cytometry is a rapidly developing modality of cytometry and is in fact the oldest form of cytometry, which traditionally presented in the form of using microscopy to subjectively observe and describe cells. Image cytometers operate by micro-photographing a large number of cells, getting whole cell information from image analysis and generating statistics of cell properties. Prior to measurement, cells are commonly labeled or stained by fluorochromes or chromatics to enhance contrast or to detect specific molecules. This technique yields visual information at the single-cell level, a type of information that is not available through other approaches. Resolution of sub-cellular structures, and analysis of cells in situ, can be achieved only by microscopy. Similarly, time-course measurements in single cells can be also obtained. Image acquisition was traditionally done manually by microscope users. Thus low statistical accuracy is one of the disadvantages of conventional microscopic measurements, since only a relatively small number of cells can be investigated within a reasonable time frame. These labor-intensive and time-consuming systems are often incompatible with high-throughput strategies.

Since the introduction of the digital camera and computational image analysis, in the mid-1990s, the automation level of image cytometers has steadily increased. This has led to the commercial availability of automated image cytometers, ranging from simple cell counters to sophisticated screening systems. Quantitative imaging cytometry is although recently introduced in the past two decades, it soon became the technology of choice for high-content (HCS), high-throughput (HTS) screening of cellular and tissue samples.

1.2 Slide-based imaging cytometric applications

The *laser-scanning cytometer* (LSC) is a representative instrument of high-content quantitative technology and is a microscope-based cytofluorometer, which has attributes of both flow cytometry and microscopy. Although having a flow cytometry heritage, it is not limited to analyzing cells in mobile fluids. In contrast, it allows automated analysis of stationary samples, including adherent cultured cells and tissues attached to microscopic slides with minimized perturbation, preserving the sample structure and vitality.

Its versatility opens up a wide range of applications, enables many cellular and tissue-based analysis throughout the biomedical sciences and pharmaceutical discovery. Fields of application may include but not limited to cell cycle analysis, immunophenotyping, quantitative histology, and cell health analysis.

Cytometric techniques have been especially applauded in pharmacology/toxicology screening. In drug discovery, for example, pharmaceutics thrive from both molecular and empirical approaches. The molecular strategies are predominantly hypothesis-driven and are referred to as target-based. The empirical approaches are referred to as phenotypic screening. An analysis has revealed the latter to be the more successful strategy.

2. Aims of study

In the era of the emerging artificial intelligence, there is a growing desire to build unbiased cytometric platforms that can harvest multiple parameters from single cells in a high throughput manner independently of the subjective human. Such platforms are exquisitely appropriate to use in histo-cyto-pathology screening, where discrepancies among human examiners should be minimized, and giving rise to a reliable diagnosis. In another significant instance, the high-content *and* high-throughput of such a platform are the essences of empirical phenotype-based screening in drug discovery.

In light of these contemporary trends, our ultimate goal is to develop and establish multiplex protocols, for both imaging cytometry and flow cytometry, which can be utilized for a broad variety of purposes. Once established, such a platform would provide scientists a ready protocol to utilize across many research and health care fields.

This dissertation aims to exemplify the adoption of LSC to characterize biological systems as demonstrated in the studies of **1**-adipocyte differentiation, **2**- DNA damage detection, **3**- protein interactions, and **4**- signaling pathways in dendritic cells.

2.1 High-content analysis of adipocyte differentiation

Currently, there is no satisfactory quantitative study about human adipogenesis that focuses on single-cell imaging cytometry, and none of them would be efficiently adaptable for high throughput applications. Here we intended to introduce a cytometry approach that could inspect adipocytes at different time points throughout their differentiation, quantitate single cells in a high-content manner yet in physiologically conservative conditions and could conveniently study both adipocytes and preadipocytes simultaneously in a slide-based platform.

2.2 LSC application for DNA damage detection

Only with slide-based technique could the cell-by-cell DNA evaluation of disrupted cells be performed with high accuracy, in contrast to flow cytometry, where necrotic debris and apoptotic bodies would disassociate away from sampled cells. In this work, we want to monitor DNA damage that occurs during normal cell differentiation using LSC.

2.3 High throughput analysis of protein-protein interactions

We aim to develop a method for semi-automated high throughput FRET measurements in LSC. Our aim was to demonstrate this by using ECFP and EYFP proteins as FRET reporters to study the interaction of Fos and Jun proteins in living adherent HeLa cells.

2.4 Elucidation of signaling pathways in a limited amount of dendritic cells

In clinical research, the limited size of obtainable sample is usually a difficult issue, this is particularly true when collecting hematological samples from pediatric patients or patients in critical conditions. By using laser scanning cytometry, we intended to show its capability to do immunophenotyping screening on dendritic cells in atopic dermatitis (AD), an inflammatory, chronically relapsing skin disorder, which affects millions of children every year.

3. Materials and Methods

3.1 Instrumental settings

The utilized LSC instrument was iCys research imaging cytometer (CompuCyte Corporation, Westwood, MA). It was equipped with three lasers (488 nm argon-ion laser, 633 nm HeNe laser, and 405 nm solid-state lasers), photodiodes (detecting light loss and scatter) and four photomultiplier tubes (PMTs). Each laser beam was shuttered under computer control. A single beam or several combined beams were steered to a computer-controlled scanning mirror that oscillates to create a scan line at the specimen. After passing through a scan lens, the beam entered the side port of an Olympus IX71 inverted microscope and focused onto the focal plane of the specimen.

The specimen carrier was mounted in a holder on a computer-controlled, motor-driven stepper stage. The stage moved in adjustable steps. Each regions of interest (ROIs) was divided into smaller areas called scan fields by the software. Each scan field (1024×768 pixels) was scanned by a focused laser beam with a step size adjustable from 0.05 to 20 μm.

3.2 Analytic softwares

The companion analyzing software iCys 7.0 (iNovator Application Development Toolkit, CompuCyte Corporation, Westwood, MA, USA) and CellProfiler (Broad Institute of MIT, MA) were used. Cellular objects or cellular organelles were automatically recognized by a process called segmentation of the image, i.e. discrimination of cells from background. Data from the cytometer was exported to FCS Express, GraphPad Prism, and Microsoft Excel, for further data evaluation and calculation.

3.3 Cell culture and differentiation induction

Simpson-Golabi-Behmel syndrome (SGBS) preadipocytes were plated in ibidi 8 well cell culture plates at a density of 15x103 cells/cm^2. Cells were cultured in DMEM-F12 medium containing 10 % FBS, 1 U/ml Penicillin, 1 U/ml Streptomycin, 0.033 µM Biotin, 0.017 µM Panthothen at 37 °C in 5 % CO_2 for 24 hours to become attached. Differentiation was induced for four days by using: DMEM-F12 with 1 U/ml Penicillin, 1 U/ml Streptomycin, 0.033 µM Biotin, 0.017 µM Panthothen, 0.1 mg/ml Apo-transferrin (Sigma), 10 µM human Insulin (Sigma), 10 µM Hydrocortisone (Sigma), 20 nM Triiodothyronine (Sigma), 1 mM Rosiglitazone (Caymen Chemicals), 2.5 µM Dexamethasone (Sigma), 25 mM 3-Isobutyl-1-methylxantin (Sigma). Medium was replaced with DMEM-F12 containing 1 U/ml Penicillin, 1 U/ml Streptomycin, 0.033 µM Biotin, 0.017 µM Panthothen, 0.1 mg/ml Apo-Transferrin (Sigma), 10-5 M human Insulin (Sigma), 10-5 M Hydrocortisone (Sigma), 20 nM Triiodo L Thyrosine (Sigma). SGBS cells were stained once with Hoechst 33342 (Hoechst 50 µg/ml, for 60 minutes, washed once). On the day of measurement, samples were stained with Nile Red (25 µg/ml) and Nile Blue (750 µg/ml) for 20 minutes.

Peripheral blood mononuclear cells (PBMCs) were obtained using Ficoll Paque Plus (GE Healthcare Bio-Sciences AB, Uppsala, Sweden) gradient centrifugation from the peripheral blood of AD patients and healthy controls. mDCs were isolated from PBMCs using the CD1c (BDCA-1)+ Dendritic Cell Isolation Kit (Miltenyi Biotec GmbH, Bergisch Gladbach, Germany). Briefly, after the depletion of CD19+ B cells, CD1c (BDCA-1)+ cells were positively selected. Purified mDCs were then cultured in RPMI-1640 medium (Miltenyi Biotec GmbH) supplemented with 10% FBS (Lonza Group Ltd, Basel, Switzerland) and antibiotics (PAA Laboratories GmbH, Pasching, Austria) for 48 hours in the presence (stimulated) or absence (unstimulated) of 30 ng/ml TSLP (eBioscience Inc., San Diego, CA, USA) and 100 ng/ml SEB (Sigma-Aldrich CO, St Louis, MO, USA).

FRET experiments were carried out using HeLa cells transfected with fluorescent proteins. Membrane proteins of HeLa were stained with Cy5 succinimidyl ester to define cell contours for segmentation of LSC data.

Primary mouse embryonic fibroblasts (PMEFs) were isolated from C57BL/6 13.5 day embryos. 3T3-L1 cells and PMEFs were maintained in Dulbecco's modified Eagle medium (with 4.5 mg/mL glucose), supplemented with 2 mM L-glutamine, 100 µg/mL Streptomycin and 100 IU/mL Penicillin in the presence of 10% Fetal Bovine Serum in 5% CO_2 at 37°C. Two day post-confluence the cells were treated with adipogenic cocktail.

3.4 Halo assay

Each well of ibidi 8-chamber slide was covered by 150 µl of 1 % LMP agarose (Boehringer Mannheim, Indianapolis, IN) melted in 39 °C. The agarose was solidified by placing the slides on ice for 2 minutes. Cells were lysed in ice-cold alkaline lysis buffer [1 % lauryl-sarcosine, 2.5 M NaCl, 10 mM Tris, 100 mM EDTA, 10 % DMSO, 1 % Triton-X-100 (pH 10)] for 10 minutes twice. Slides were neutralized and washed in cold 1x PBS with 5 µM EDTA buffer (pH 7.4) for 4x 4 minutes and fixed in cold 1 % formaldehyde for 4 minutes. The slides were stained with SYBR Gold (Molecular Probes, Eugene, OR) diluted 1:10000 in TE [10 mM Tris (pH 8.0) and 2 mM EDTA] for 15 minutes. Cellular event before and after lysis was computationally traced object-by-object to associate DNA halo with its original parent cell. Multiple thresholds were applied to analyze SYBR Gold signal, nucleoid matrix was distinguished from migrated DNA in halo ring. Consequently, *Tau*, a parameter monitoring DNA damage, was defined as the fraction of DNA migrated to the periphery of the original nucleus ("halo") over the total DNA integral of a cell.

3.5 Data acquisition and texture analysis for adipocytes

405-nm Violet diode laser excited Hoechst 33342, 488-nm Argon-ion laser excited FITC, Nile Red and propidium iodide, 633-nm HeNe gas laser excited Nile Blue. Hoechst was detected at 463±20 nm, FITC at 530±15 nm, Nile Red at 580±15 nm, propidium iodide and Nile Blue at 675±25 nm. Transmitted laser light was captured by diode photodetectors in which light loss and shaded relief signals were measured to gain light absorption, scattering and textural characteristics of the objects. Entropy measures the randomness of intensity distribution: sum entropy (ΣE) roughly informs about the number of lipid droplets. Parameter Variance measures the difference between intensity of the central pixel and its neighborhood: sum variance (ΣV) roughly depicts the size of lipid droplets.

3.6 Data acquisition for FRET

405-nm solid-state laser, 488-nm Argon laser and 633-nm HeNe laser excite ECFP, EYFP, and Cy5, respectively. The autofocus utility determined the inclination of the cover slip by triangulation. During the scan, a fixed offset from the bottom of the cover slip was applied, which placed the focus to the middle plane of cells. Laser intensities at the objective were 151 µW for the 405-nm and 27 µW for the 488-nm lines. Donor and transfer signals were collected through 460-500 and 520-580 nm band-pass filters by separate PMTs; the acceptor was detected at 520-580 nm by the same PMT as the transfer signal; Cy5 fluorescence was detected through a 650-nm long-pass filter.

Raw scanned images were processed post-acquisition by the CellProfiler software, and pixel-by-pixel FRET calculations were carried out according to equations described in section 4.3.

4. Results

4.1 High-content analysis of human adipocyte differentiation

4.1.1 Advanced algorithm for high-content data acquisition from human adipocyte cultures

A high-content analysis with advanced algorithms was designed and optimized to identify accurately crowded cells in highly confluent adipocyte cultures. Fluorescent signals from multiple channels were analyzed both in separate and conjoint mode. Hoechst stained nuclei were contoured when the signal exceeded a preset threshold value using *adaptive Otsu threshold*. Throughout cell auto-detection, nuclei of cells were firstly identified and marked as *primary* objects, based on which the *secondary* objects were later recognized: Adipocytes were segmented if fluorescence signals of lipid droplet specific Nile Red was higher than the background. Preadipocytes were subsequently segmented based on the intensity of phospholipid specific Nile Blue fluorescence. This two-step process minimized the existence of non-cellular events in data evaluation. We compared our segmentation result to currently available methods as well as to ground-truth segmentation by human manual contouring. Accuracy, which is the proportion of the true prediction achieved by the segmentation, and F-measure, which is a more widely used statistical parameter to evaluate imaging algorithms, were calculated. Both parameters ranked our method higher.

The differentiation model was designed and inspected for a period spanning 15 days, during which imaging cytometric assays of live cells cultured in ibidi chamber-slides were performed along two parallel courses of study: either sequential substitutes or longitudinal follow-ups. With the former design, a similarly induced group of fresh SGBS cells was divided into subgroups, which were then placed on separate slides; each subgroup was allowed to grow in incubator until its scheduled daily measurement. On the other design, a particular sample was studied in a cohort pattern where cellular changes were tracked on cell-by-cell basis. Both series served to clarify how cellular morphology and lipid content changes at each time point during the progression of the differentiation.

4.1.2 Inspection of adipocyte differentiation using organelle-specific dyes and texture analysis

Fluorescence intensities of fluorochromes, light absorption, area (bounded by the contour line in square micrometer), and texture parameters were used to assess lipid accumulation, cell and nuclear size alterations, DNA content and cell phases. Classification of differentiation stages was

relied on Nile Red-staining, texture properties of light loss, and nuclear condensation. This auto-classification was supervised by visual identification of cellular events after relocating them. Cells that contained lipid accumulation (Nile Red, texture variance and entropy) above a preset threshold value were considered differentiated adipocyte. The ratio of number of adipocytes over the total count of nuclei gave rise to differentiation ratio, calculated in a region of at least 100 field images per sample. The combination of multi-parameters significantly improved the assessment of differentiation stages compared to conventional quantification using only lipid fluorescent staining.

Along the differentiation, characteristic texture was identified in undifferentiated cells, committed differentiating preadipocytes, and terminally differentiated adipocytes. Strong correlation between texture properties and fluorescence from lipid accumulation was found. The increase in texture parameter sum entropy in parallel with lipid droplet accumulation was elucidated during the differentiation from preadipocytes to adipocytes. Preadipocytes showed lower sum entropy and sum variance of texture compared to adipocytes. Benefiting from these two texture parameters, discrimination between preadipocyte and adipocyte populations was more robust than using only Nile Red fluorescence. All texture parameter alterations mainly originated from cellular roughness and granularity changes detected via transmitted (and scatter) light signals.

The preadipocyte commitment was found to occur on day 2-3 with a compacting cytoplasm, revealed by increasing light-loss signal. At this point, forming lipid structures still did not stain with Nile Red (triglyceride) but only with Nile Blue (phospholipid). Shortly after, day 4-5, minor but measurable Nile Red signal appeared. A relatively few small separated lipid droplets and an enhanced nuclear condensation were shown in committed preadipocytes on day 2-5. This was in contrast to undifferentiated cells, which had more cytoplasm, round giant and faintly stained nuclei with no Nile Red fluorescence. From day 6 to day 12 most of the adipocytes reflected typical morphological signs of *in vitro*-differentiated adipose cells, such as round distending shape, a cytoplasm filled with lipid droplets as well as strong Nile Red fluorescence and light-loss signals. Shrinking and more brightly stained nuclei, signs of nuclear condensation, became even more pronounced. At day 9-12, when the ratio of fully differentiated cells reached 40% in the region of optimal confluence (two-dimensional in vitro confluence), the differentiation curve was considered saturated. Indeed, from day 12 until the completion of the experimental regime (18 days), no further formation of lipid droplets was seen, rather the lipid droplets fused together and became distorted.

4.1.3 Detection and quantification of apoptosis in pre-adipocytes and adipocytes

Spontaneous and induced apoptosis was assessed by a multi-step assay. Before apoptosis induction, a region of interest (ROI) was determined by mosaic scan, where most of adipocytes were located, this region was scanned once to obtain pre-treated control (first scan layer). Next, apoptosis induction was applied and a scan was performed upon same ROI using exactly the same instrumental setup (second scan layer). Lastly, the sample underwent a halo assay where nuclei were examined for DNA fragmentation and a third layer of scan was performed on same ROIs. Merging image data of these three layers gave rise to the correlated data at different experimental phases, i.e. before and after treatments.

On every third day of the differentiation period, apoptosis induction was conducted on preadipocytes and adipocytes using TNFα treatment. Apoptotic ratio was defined as number of Annexin V positive cells over the total count of Hoechst stained nuclei. Before TNFα treatment, Annexin V labeled cells in the first scan layer represented spontaneous apoptosis, whereas AV+ cells in the second scan layer, recorded after the TNFα treatment, indicated the induced apoptosis. Merged first and second layer gave individual information of each particular cell on how it progressed through the apoptosis induction. Merging of layers means that images taken before and after apoptosis induction were computationally stacked over each other to allow correlation analyses of cellular information from exactly the same cells before and after the treatment.

We observed a stable spontaneous apoptotic rate in both adipocytes and their precursors, ranging from 7.05 % to 17.91 %. After apoptosis induction, significant increase of Annexin V and propidium iodide positivity were seen in both cell types at every time point of differentiation. Particularly, preadipocytes showed more sensitivity to the apoptosis induction, as 26.06 % to 50.09 % of preadipocytes showed Annexin V positivity compared to that of 30 % average in the adipocyte population.

Additionally, the apoptosis induction brought on apoptotic bodies, which showed highly fragmented DNA in halo assay as well as strong fluorescence of Hoechst intensity. Typical membrane blebs in close association with condensed nuclei were observed in the majority of apoptotic cells. There was remarkable cell loss, which was proportional to the percentage of cells responded to the apoptosis induction: 24.12 % ± 10.5 % of cells was lost in induced samples compared to 10.67 % ± 4.52 % in controls (from data comparing nuclei counts before and after treatment in day-12 samples).

4.2 DNA damage detection in different cell fates and cell lines

A quantification of nuclear size and shape at population level confirmed that: in preadipocytes, large nuclear size was found to correlate with fainter Hoechst stained DNA, while adipocytes showed more compact nuclei and brighter Hoechst intensity. This significant nuclear condensation lead us to the hypothesis of DNA fragmentation may take place at a certain degree to facilitate such a crucial cellular program as terminal differentiation. Suggestively, other studies in myogenesis have demonstrated that possible involvement of caspase-activated DNAse during cell differentiation. It has also been reported that the lack of caspase 3 activation or dysfunction of CAD stop muscle differentiation, furthermore DNA damage was detected during the otherwise normal process. The DNA detecting assay was thus performed at each inspected time point of differentiation to estimate possible DNA damage.

Halo assay

We developed a screening assay that can systematically examine the level of DNA damage in cells of different tissue origins and under different conditions. We adapted a modification of the comet assay, called the "halo" assay. Using this assay, the damaged DNA forms a halo around the undamaged DNA in the center because the electrophoresis step is omitted. We introduced a new parameter, *Tau*, in order to quantify DNA damage by halo assay using standard LSC software.

$$Tau = \frac{FI_{Halo\ Ring}}{FI_{Total\ Halo}}$$

where $FI_{Halo\ Ring}$ is the integrated fluorescence in the peripheral halo, $FI_{Total\ Halo}$ is the integrated DNA fluorescence of the matching nucleus. *Tau* was thus a quantitative entity, linearly proportional to DNA damage. This allows direct quantification of DNA fragmentation using the parameters collected by the LSC.

4.2.1 Accumulating DNA damage was seen during SGBS adipocyte differentiation

To quantify DNA fragmentation, DNA was stained with SYBR Gold after being lyzed in halo assay. In healthy cells, DNA fluorescence of a halo was confined to the center of nuclei since unfragmented high molecular weight DNA diffuse out at proximal distance. In cells that had more DNA damage, smaller fragments migrated further from the central nucleoid matrix. Fluorescent signals of total integrated DNA were collected by a lower segmentation threshold in; whereas fluorescent signals within nucleoid matrix were collected by a higher threshold. The halo ring, which was the region between two contoured thresholds, was subsequently segmented.

We found that, the *Tau* value of Annexin V-negative cell population rose from 0.16 to 0.27 on day 3, and at day 5, its value plateaued at 0.4, indicating a spontaneous increase of DNA fragmentation during the differentiation process. This finding, as an original observation on single cell level, suggests that spontaneous DNA fragmentation occurs during adipocyte differentiation in the absence of apoptosis.

4.2.2 Accumulating DNA damage was also observed during mouse adipocyte differentiation

We also inspected the case of DNA damage propagation during adipogenic differentiation in other species, namely mouse adipogenic differentiation, using the conventional mouse 3T3-L1 adipocyte cell line, mouse embryonic stem cells (MESC) and primary mouse embryonic fibroblasts (PMEF). There was repetitive evidence of DNA damage (high Tau) in AV-negative differentiated population of all tested cell lines. The confirmative results indeed strengthen and generalize the phenomenon seen in human SGBS cell line. To the best of our knowledge, our work is the first study that reports DNA damage in human adipocyte differentiation.

4.3 Protein-protein interactions as studied by FRET

We demonstrated here the stable heterodimer formation of Fos and Jun in nanometer scale by analyzing FRET in a protein fusion design: CFP-tagged Fos and YFP-tagged Jun. LSC was used for the identification of FRET in adherent, ECFP-EYFP double-positive HeLa cells.

To determine the apparent FRET efficiency value (*E*) in a large number of attached cells, we intended to build a ratiometric protocol to be executed in a high throughput fashion. However, FRET efficiency calculation by ratiometric FRET requires the instrumental correction factor α. Therefore, we constructed an additional LSC protocol to gain E_{Pb} FRET efficiency and derive consequently the correction factor α from E_{Pb}. With gained α, desirable high-throughput ratiometric protocol could be then performed. The two intertwined protocols provided all necessary parameters for FRET determination and thus gave LSC system an independent capacity to measure protein-protein interaction without the aid from other instruments.

It is essential to include only living cells in evaluation of FRET efficiency. To avoid complication of fluorescent interferences in FRET calculation, we minimized the number of staining dyes and thus did not use specific staining that could discriminate viable and dead cells, i.e. membrane or nuclear staining that is sensitive for detection of apoptotic or necrotic cells.

We used the membrane impermeable Cy5 succinimidyl ester fluorescent dye for recognizing cellular objects. It also helped discriminate live and dead cells based on Cy5 intensity, since Cy5

bonded covalently to primary amine groups of proteins at the cell surface of living cells whilst it penetrated into dead cells. Furthermore, we used cell axial length and texture as other parameters to exclude unacceptable cells. Adherent HeLa cells usually possess filopodia, thus have a clear difference between the lengths of the major and minor axes. Floating detached cells obviously featured rounded shape with equal axes. Cells that had blebbing or ruptured membrane often possessed a more granular texture.

The entities in FRET evaluation included the unquenched donor intensity (I_D), the acceptor intensity without FRET (I_A), the FRET efficiency (E), the spectral crosstalks (S_1-S_3), and fluorescence efficiency instrumental (α) factor, and were described by the following equations for LSC:

$$I_1 = I_D(1 - E) \tag{1}$$

$$I_2 = I_D(1 - E)S_1 + I_A S_2 + I_D E\alpha \tag{2}$$

$$I_3 = I_D(1 - E)S_3 + I_A + I_D E\alpha \frac{\varepsilon_4}{S_2} \tag{3}$$

These equations were then solved for the apparent FRET efficiency, *E*:

$$E = \frac{I_2 - I_1 S_1 - I_3 S_2 + I_1 S_2 S_3}{\alpha(1 - \varepsilon_4)I_1 + I_2 - I_1 S_1 - I_3 S_2 + I_1 S_2 S_3} \tag{4}$$

where S_1, S_2, and S_3 were spectral crosstalk between the channels, defined as:

$$S_1 = \frac{I_2}{I_1} \tag{5}$$

$$S_3 = \frac{I_3}{I_1} \tag{6}$$

calculated from a donor-only labeled sample, and

$$S_2 = \frac{I_2}{I_3} \tag{7}$$

calculated from an acceptor-only labeled sample.

The term ε_4 is a ratio of the extinction coefficients of ECFP and EYFP at the wavelengths used for exciting the donor (405 nm) and the acceptor (488 nm):

$$\varepsilon_4 = \frac{\varepsilon_{488}^{ECFP}\varepsilon_{405}^{EYFP}}{\varepsilon_{405}^{ECFP}\varepsilon_{488}^{EYFP}} \quad (8)$$

In our case, $\varepsilon_4 = 0.00978$.

The expression of α was as follows (9):

$$\beta = I_2 - I_1S_1 - I_3S_2 + I_1S_2S_3$$

$$\alpha = \frac{\frac{\beta}{E} - \beta}{(1-\varepsilon_4)I_1}$$

In donor photobleaching results, ECFP-EYFP fusion sample showed significantly longer exponential decay of intensity (slower bleaching kinetics) than that of both the ECFP only and the ECFP and EYFP co-transfected sample. This indicated the presence of FRET in fusion sample, reflecting the close molecular proximity of FRET proteins. Energy transfer efficiency for the positive control of ECFP-EYFP fusion sample was ~40%, between 36-52%, when calculated from the measured τ_D and τ_{DA} bleaching time constants. The negative control ECFP and EYFP co-transfected sample remained below 5%, closer to 0%. The positive control also delivered an average *E* value to feed ratiometric equations, by which *α* factor for the LSC was achieved.

When continuing with ratiometric measurements, the average of *E* for the positive control was close to 40%, while in the negative control around 0%. For the double-transfected sample Fos-CFP+Jun-YFP, *E* above 5% was accepted as significant value of fluorescence energy transfer efficiency. This value reflected the molecular proximity of the donor and acceptor, and thus indicated that the tagging proteins were closer than 10 nm, the critical limit of the FRET. This also offered a good expectancy for the molecular intimacy of the tagged proteins.

With ratiometric FRET, we gained information from the population distribution of *E* in single cells. For instance, we recognized a subpopulation of cells where Fos and Jun heterodimerize since there was a significant *E* present and another subpopulation where Fos-Jun heterodimerization was missing or different. However, we have to note that the *E* value measured in a single cell was an average value or an apparent transfer efficiency. It came from many FRET partners with different separation distances and/or from different ratio of the donor and acceptor fluorophores.

We also acquired knowledge about the pixel-by-pixel subcellular distribution of FRET efficiency harnessing ratiometric FRET by LSC. In our situation, the heterodimerizing Fos-CFP and Jun-YFP accumulated in nucleus, where they gave significantly high FRET efficiency, while in the positive control sample (CFP-YFP fusion), high *E* value originated from both the nucleus and the cytoplasm.

4.4 LSC application on studying T helper cell polarization of dendritic cells

In atopic dermatitis (AD), myeloid dendritic cells (mDCs) are actively involved in the initiation and lineage commitment of several skin-infiltrating T helper (Th) subpopulations. In turn, mDCs are tightly controlled by tissue microenvironment of the skin. Characteristic features of the skin microenvironment include skin colonization with superantigen-producing Staphylococcus aureus, which correlates with the severity of the disease, and the presence of Staphylococcal enterotoxin B (SEB) and thymic stromal lymphopoietin (TSLP), which is strongly overproduced by keratinocytes in lesional and non-lesional skin due to skin barrier dysfunction.

Due to the restricted availability of the clinical samples and limited number of cells per sample from pediatric individuals, we designed our measurement using LSC instead of flow cytometry (11 atopic patients, yielding about 1 million DCs each sampling). The study had been conducted with the major contribution of Department of Dermatology and Department of Dermatological Allergology, University of Debrecen Medical and Health Science Centre, Debrecen, Hungary.

As shown by the research group, the atopic skin-like microenvironment could modulate the T cell-polarizing cytokine production of myeloid DCs. Upon SEB-TSLP dual stimulation, myeloid DCs from AD patients responded by a significant expression of CD83 and CD86. Dendritic cells activated by SEB-TSLP were shown to express cytokines that favor the predominance of Th2 and Th22 subtype.

In AD patients, we reported a high fraction of cells with decondensed chromatin accompanied with increased cytokine expressions. After stimulation, a significant up-regulation of CD83 and CD86 was found, accompanied by further chromatin decondensation, which may imply active transcriptions of dendritic cells.

5. Discussion

5.1 Discussion for subsection 4.1- "High content analysis of adipocyte differentiation"

Application of LSC to fat cell analysis

Amongst vast variety of methods to investigate adipocyte biology, genetic approaches, biochemical assays, flow cytometry and conventional microscopy are most commonly used. Although biochemical techniques have largely contributed in understanding adipogenesis and adipoapotosis, it is incomplete to resolve potential heterogeneity of cell populations following a bulk analysis. While common microscopic methods are able to study single cells, their subjective application is user dependent and thus lacks of unbiased quantifications. Flow cytometry has the advantage of being quantitative on single cell level, but it too has inherent shortcomings stemming from its design: handling samples in tubes and lifting cells in suspension.

In our case living adipocytes were cultured in chamber-slides along the entire experiment and measurement; this was especially useful for our follow-up studies of time-resolved differentiation and apoptotic destruction processes. Morphological properties of individual cells as well as stoichiometric data of large populations were inspected and interrogated with minimized perturbation. Plotted data points were also relocated and examined by visualization and thus improved time-lapse experiments with live subjects.

Improved protocol for automated cell segmentation

In slide-based histo-cytometric system, advanced imaging processing is required to enable cell-by-cell analysis in highly confluent samples. When facing this challenge, McDonough et al. have introduced tessellation algorithm that could estimate the boundaries between the cells. Still, this procedure would only be valuable when lipid droplets in adipocytes are closely associated with a centric nucleus, which is not always valid since mature adipocytes have typical eccentric nuclei. On the other hand, tessellation generates pseudo-cell boundaries, i.e. instead of selectively propagating from foreground pixels, the whole image is segmented, and thus collected data would avoidably include background pixels. In our case, we utilized CellProfiler image analysis software with customizable adaptive Otsu's segmentation and declumping algorithm constituting of two-step object identification (*primary* and *secondary)*. This protocol has improved cell recognition, cell contouring, and led to a more precise quantitative data acquisition at high cell density of adipocytes. Thus, this work introduced a reproducible and information-rich protocol to follow the differentiation process of preadipocytes to adipocytes from the same SGBS cell population.

Employing texture properties significantly improved adipocyte identification

Beside fluorescent intensity profiles as in conventional imaging microscopy, in this work texture properties of cellular objects were also analyzed and were demonstrated to be an improved approach to investigate morphology of a mixed population of undifferentiated cells, preadipocytes, and white adipocytes.

In flow cytometry, light scatter is generally used for event recognition but forward (FSC) and side scatter (SSC) signals are also valuable parameters to resolve size and granularity of cellular objects. In LSC technology, transmitted light was captured by diode photodetectors in which light loss and shaded relief signals were measured to gain information about light absorption and scattering characteristics of the objects, respectively. LSC allowed defining several computed texture parameters of image data with absorption and scattering signals. The computational freedom of texture properties of cells proved to be beneficial and gave rich information.

We have used two texture parameters: entropy and variance, which informed us about number and size of formed lipid droplets, respectively. When using these parameters to interpret adipocyte differentiation, we have recognized that these parameters were rather more sensitive or at least give similar results to signals based on conventional fluorescent or chromatic lipid droplet dyes or Nile Red in our instance. In harmony with us, other study found that side scatter granularity signal in flow cytometry efficiently recognized lipid droplet formation of mature adipocytes differentiated from 3T3-L1 cells. We have broadened their application to slide-based cytometry, where texture parameters provided improved signals for early identification of lipid droplet formation.

Adipogenesis undergoes two stages

The observation that most adipocytes completed terminal differentiation on day 10-12 coincided well with the generally accepted time point when adipocytes were considered fully differentiated. Our results were also in favor of the concept of two stages in adipogenesis: the initial commitment of mesenchymal stem cells to a preadipocyte fate and then terminal differentiation.

5.2 Discussion for subsection 4.2 - "Detection of DNA damage during differentiation"

Nuclear condensation during human adipocyte differentiation

Level of lamin A and B proteins have been reported to decrease at peripheral regions of nuclei during adipocyte differentiation, while vimentin reorganized into cage-like structures near lipid droplets. These observations were noted at the same phase of adipocyte transformation

identified by us, in which the shrinkage of the size of nuclei along with the increasing intensity of DNA staining were recognized. We suggest that these morphological changes may be the different phenotypical presentations of the same molecular modulation happening together with chromatin condensation.

Increased DNA fragmentation during human adipocyte differentiation

We have observed that *Tau*, indicating level of DNA damage, was continuously increasing from day 3, an early time point even preceding the initiation of texture parameter increase or lipid droplet formation. In murine 3T3-T preadipocytes, other work previously showed that DNA repair capacity was reduced during the differentiation program. However, conflicting data has recently risen regarding the repair of double strand breaks in adipocytes, in which a specific DNA repair mechanism for double strand break was shown to be increased. Nevertheless, in all of these works DNA damage was monitored in bulk samples, where it was unable to resolve changes on single cell level. Our study introduced, for the first time, the detection of direct DNA damage in single cells during the adipogenesis. Conflicting data mentioned above might originate from heterogeneous populations with double strand breaks emerging in adipogenesis. These potentially heterogeneous subpopulations might carry different capacity towards various DNA repair routes. This issue might be resolved by our method if direct single and double strand breaks would be measured specifically in single cells.

Accumulation of DNA damage or decrease of capacity of complete replication of genome seems to be a sign of differentiation of somatic cells in multicellular organisms. Caspase 3 has been shown in different studies to play an important role in a variety of activation of tissue differentiation. It was observed in the differentiation of skeletal muscle, caspase 3 activates CAD, and is linked to the p21 promoter as one crucial step in the normal differentiation. In addition, it has also been reported that the lack of caspase 3 activation or dysfunction of CAD stop muscle differentiation, furthermore DNA damage is detected during the otherwise normal process. Another interesting report is that FasL and TRAIL- activated apoptosis produce mutagenesis in surviving cells via CAD-mediated effects.

We believe that increasing level of average DNA damage we have observed with alkaline halo assay or a possible heterogeneity in developing DNA damage in maturing non-apoptotic SGBS cells is a part of this general phenomenon. We are continuing our work in this field to resolve this possibility.

5.3 Discussion for subsection 4.3 - "High throughput screening of protein-protein interaction"

In this work, a ratiometric FRET protocol specifically designed for laser-scanning cytometry (LSC) was presented. The procedure was aimed to evaluate protein-protein proximities by determining the energy transfer efficiency (*E*) value in large number of attached cells. We showed that ECFP and EYFP fluorescence could be detected with sufficiently high sensitivity and accuracy. We compared FRET results obtained with a confocal laser scanning microscope having optimal excitation wavelengths for the excitation of ECFP and EYFP (458 and 514 nm) with results gained from the LSC and a flow cytometer, both having suboptimal excitation wavelengths (405 and 488 nm), (data not shown). By using an ECFP-EYFP fusion protein as a standard, FRET efficiencies measured between Fos and Jun proteins using the different instruments were nearly identical.

Furthermore, we have developed a method to measure absolute FRET efficiencies using only the LSC. In our scenario, ratiometric measurements required an instrumental correction factor α to determine ahead of the other experiments. We successfully developed a donor photobleaching FRET measurement with LSC to determine *E*, independent from the ratiometric protocol. Using the consensus *E*, this procedure made the determination of α possible.

A limitation of intensity based FRET methods was that they could not resolve donor-acceptor subpopulations characterized by different individual *E* values. The measured apparent *E* value was conventionally an average over individual FRET efficiencies arising from different donors in the cell or in the observation area. Here we demonstrated a solution by using pixel-by-pixel map of FRET efficiencies on a cell-wise measurement.

We defined the methodology for semi-automated FRET measurements uniting the high throughput of cytometric FRET with the capability of subcellular localization and cell backtracking in a single instrument. Our method can facilitate screening of protein interactions with both statistically relevance and the sub-cellular pixel-by pixel resolution.

5.4 Discussion for subsection 4.4 -"T-helper polarization of dendritics in atopic dermatitis"

We suggest that circulating mDCs have a pluripotent ability to polarize all types of Th cells both in AD and in healthy individuals. In the presence of the disease specific environmental stimuli, they further exhibit characteristic polarizing cytokine patterns secondarily in the skin.

The amount of dendritic cell that could be obtained from clinical patients is generally limited. In this particular study, this limitation is a major obstacle, where the conventional flow cytometric method of investigation is not suitable. Thus, the utilization LSC was proven sufficient to study the effect of new DC-targeted therapeutic modalities in AD.

5.5 General discussion and conclusions

The terms High-Content Imaging and High-Throughput Screening were introduced more than a decade ago and ever since have gained significant momentum due to its ability to study many features simultaneously in complex biological systems. They define the use of automated microscopy and automated image analytical paradigm to achieve answers for biological questions. Clearly, those technologies are expected to improve significantly phenotypic cellular assays by generating relevant and multi-parametric data sets without laborious works.

From this perspective, our work has been developed based on a laser-scanning cytometry platform. Our presented slide-based demonstrations showed strong capacity to satisfy both unbiased reliability and high-throughput performance. In these works, we utilized the combination of a slide-based scanning platform and image analysis softwares to generate "flow cytometry"-like data, based on high content imaging. This system was capable of being programmed and user can design automated measurements as well as semi-automated analytic procedures, either prior or after measuring the samples. This allowed both automatic acquisition of visual information of cells or tissues and reducing the laborious maneuvers on conventional microscopes.

Analytical companion softwares purchased with the scanning instrumentations usually have restricted capabilities. General options of such default analytical softwares might provide good data mining tools for easy cellular events and objects, such as round cells, clearly distinguishable objects, samples with optimal cell density or concentration, tissue sections with homogenous staining, samples with clearly visible and detectable signals, high signal to noise ratio etc. However, each specific study might bring new challenge; for instance: study dealing with cells that require culture in high confluence, cells possessing extensive processes (e.g. filopodia), mobile or dividing cells, cells

changing size and shape, and especially, unpredictable responses to various treatments, where features of interest before and after the treatments are required to be recorded and inspected.

Thus, a more complex algorithm to facilitate such specific study is largely demanded. Here, we demonstrated our success in developing:

- Multi-step image segmentation to improve cell recognition in heterogeneous, attached cell culture at high confluence.
- Development of texture analysis as a new parameter to study cell morphology and cell differentiation.
- Combination of vital and non-vital imaging and analysis to evaluate cell differentiation and concomitant DNA damage.
- Cyclic, time-lapse, and tracking measurement to study protein interactions by FRET.
- Solution to overcome the insufficient procurement of cells in small clinical samples.

We could assess multiple morphological and functional features of both individual cells and cell populations, and the exported stoichiometric data could undergo further mathematical and statistical evaluation procedures. We have shown that our slide-based cytometric approach could make valuable observations in different cell types, cell lines, and treatments. Such achievement on high-content data was based on the detection of total cell signal, where signals were acquired by photomultipliers from the whole depth of the cell, without using confocal pinhole.

Performing image analysis for high-content screening requires a strong computational power. Both imaging acquisition, imaging analyzing and data generating processes are time- and resource-consuming, which can restrict multiparametric analysis. This restriction in turn is the main factor that balances between the high-throughput and high-content modality our system. For instance, one fundamental factor affecting the throughput is the time of imaging. When cellular and sub-cellular details are required in high quality, one needs to optimize the exposure time and magnification. Depending on the size and confluence of cells on slide, the size of each viewing field image consequently controls the number of images to acquire per well. This can deeply influence the processing time in a scenario where a large area of the whole 96-well plate is needed to be scanned. The duration of the screening campaign therefore can be too long for living subjects. During such long duration, cells may undergo morphological changes and adversely affect the quality of the scan.

Unfortunately, scanning cytometry also requires a well-trained operator to eliminate the effect of the small physical misalignments that happens during measurements, e.g. when sample

holders are replaced, stages are moved, or objectives are changed. Such misalignments can dramatically affect the repetition of automatic cell identification, thus influence assigned analytical values of the investigations.

The implementation of complex assays exploiting primary cells, live cell imaging (time-lapse), cell migration or 3D imaging in a real high-throughput format, is still a tempting goal.

In addition, improved analytical systems, “soft-wares”, with more precision and automation are indeed drawing more attention than a further improvement of “hardware” instrumentation. Self-learning machine and human-independent analyses have been long a central target of algorithmic studies.

This approach can be potentially expanded to evolve into a more complex and powerful research modality combining gene expression data with cytometric analysis, and quantitative immunohistochemistry with the resolution of organelle specific markers. Once established, such platform would provide scientists an artificial-intelligent advisory system with ready protocols to utilize across many research and health care areas.

6. Key words:

High content screening, High throughput screening, High content analysis, imaging cytometry, laser scanning cytometry, quantitative cytometry, adipocyte, adipogenesis, DNA damage, DNA break, halo assay, comet assay, FRET, protein interaction, dendritic cell

7. Summary

The dissertation provides an overview of advancements in high-content screening techniques, with special focus on slide-based imaging cytometry. Contemporary studies that utilized this technology have been highlighted. The review has discussed both the significances, benefits as well as limitations of high-content and high-throughput analyses in different investigations, namely cell cycle analysis, immunophenotyping, quantitative histo-cyto-pathology, cell health analysis, and pharmacology/toxicology.

In addition to the review sections, the thesis has also demonstrated four studies that were conducted by the author and his collaborations: High-content analysis of adipocyte differentiation; High-throughput screening of protein-protein interactions; Detection of DNA damage in differentiating cells; and Study of polarization signaling pathway in dendritics.

These studies exemplified the successful adoptions of laser scanning cytometry into studying cell biology. Moreover, these studies have shown valuable results with both methodological and biological significance. Namely, the author has shown improved cell recognition in heterogeneous, attached cell culture at high confluence; the valuable application of textural analysis in inspection of cellular morphology; pixel-by-pixel FRET map of protein heterodimerization in large number of attached cells; and proofs of the accumulation of low-grade DNA damage during cell differentiation.

The demonstrated applications belong to various orientations and are indeed excellent representatives of objective quantitative cytometry. The establishment of such useful screening platform of the workgroup is encouraging and of great potential, which can effectively serve multiple purposes across different research fields in biology and health cares.

8. Acknowledgment

I have never enjoyed a task more than spending time with and learning from the Biophysics and Cell Biology Department members in University of Debrecen.

I am forever indebted to Dr. Zsolt Bacsó for his devoted coaching, limitless tolerance, and patience. I had the unique honor of having trained under his instruction and of many other Professors and Teachers of Biophysics University of Debrecen since 2004. They have taught me much about the science and the art of medicine. I feel that I have stood in the shadow of giants. I sincerely appreciate Prof. Gábor Szabó, Prof. János Szöllősi and Prof. László Fésüs for giving me the opportunities and kind supports to initiate my scientific career.

I am extremely grateful to Szalóki Nikoletta, Kristóf Endre Károly, Anitta Kinga Sarvari, Georgina Nagy, Cimmerer Zsolt and Ixchelt Cuaranta-Monroy for their friendly and productive collaboration.

Despite being far away, my family has always been unwavering in their supports. Many other dear friends have also given me endless encouragements.

The completion of this project would not have been possible without the expertise and devotion of all of you.

Doan Xuan Quang Minh.

This work was performed by support from the Hungarian Scientific Research Fund Grants: OTKA K77600, K103965, NK 101337, K75752, CK78179, NK105046, OMFB-01626/2006; the New Hungary Development Plan grants: TÁMOP-4.2.1/B-09/1/KONV-2010-0007, TÁMOP-4.2.2/B-10/1-2010-0024, TÁMOP-4.2.2.A-11/1/KONV-2012-0023, TÁMOP-4.2.2.A-11/1/KONV-2012-0025; and the Baross Gábor Program (REG-EA-09-1-2009-0010).

Register number: DEENKÉTK/367/2014.
Item number:
Subject: Ph.D. List of Publications

Candidate: Quang-Minh Doan-Xuan
Neptun ID: T6X3ZN
Doctoral School: Doctoral School of Molecular Cell and Immune Biology

List of publications related to the dissertation

1. **Doan-Xuan, Q.**, Szalóki, N., Tóth, K., Szöllősi, J., Bacsó, Z., Vámosi, G.: FRET Imaging by Laser Scanning Cytometry on Large Populations of Adherent Cells.
Curr. Protoc. Cytom. Suppl. 70., 1-29, 2014.
DOI: http://dx.doi.org/10.1002/0471142956.cy0223s70

Doan-Xuan, Q. and Szalóki, N. contributed equally to this article.

2. Szalóki, N., **Doan-Xuan, Q.M.**, Szöllősi, J., Tóth, K., Vámosi, G., Bacsó, Z.: High throughput FRET analysis of protein-protein interactions by slide-based imaging laser scanning cytometry.
Cytometry A. 83 (9), 818-829, 2013.
DOI: http://dx.doi.org/10.1002/cyto.a.22315
IF:3.066

Szalóki, N. and Doan-Xuan, Q. M. contributed equally to this article.

3. **Doan-Xuan, Q.M.**, Sárvári, A.K., Fischer-Posovszky, P., Wabitsch, M., Balajthy, Z., Fésüs, L., Bacsó, Z.: High content analysis of differentiation and cell death in human adipocytes.
Cytom. Part A. 83 (10), 933-943, 2013.
DOI: http://dx.doi.org/10.1002/cyto.a.22333
IF:3.066

Doan-Xuan, Q. M. and Sárvári, A. K. contributed equally to this article.

List of other publications

4. Cuaranta-Monroy, I., Simándi, Z., Kolostyák, Z., **Doan-Xuan, Q.**, Póliska, S., Horváth, A., Nagy, G., Bacsó, Z., Nagy, L.: Highly efficient differentiation of embryonic stem cells into adipocytes by ascorbic acid.
Stem Cell Res. 13 (1), 88-97, 2014.
DOI: http://dx.doi.org/10.1016/j.scr.2014.04.015
IF:3.912 (2013)

5. Nagy, G., **Doan-Xuan, Q.**, Gáspár, K., Mócsai, G., Kapitány, A., Törőcsik, D., Bacsó, Z., Gyimesi, E., Remenyik, É., Bíró, T., Szegedi, A.: The atopic skin-like microenvironment modulates the T-cell-polarising cytokine production of myeloid dendritic cells, as determined by laser scanning cytometry.
Exp. Dermatol. 23 (4), 276-278, 2014.
DOI: http://dx.doi.org/10.1111/exd.12342
IF:4.115 (2013)

6. Székvölgyi, L., Imre, L., **Doan Xuan, Q.M.**, Hegedűs, É., Bacsó, Z., Szabó, G.: Flow Cytometric and Laser Scanning Microscopic Approaches in Epigenetics Research.
Methods Mol. Biol. 567, 99-111, 2009.
DOI: http://dx.doi.org/10.1007/978-1-60327-414-2_7

Total IF of journals (all publications): 14,159
Total IF of journals (publications related to the dissertation): 6,132

The Candidate's publication data submitted to the iDEa Tudóstér have been validated by DEENK on the basis of Web of Science, Scopus and Journal Citation Report (Impact Factor) databases.

08 January, 2015

10. Appendix

Other publications related to dissertation:

Abstract:

Doan-Xuan, Q.-M., Szalóki, N., Tóth, K., Szöllősi, J., Bacso, Z. and Vámosi, G. Förster resonance energy transfer analysis of nuclear proteins by laser scanning cytometry.
Eur Biophys J (2011) 40 (Suppl 1):S35–S241, DOI 10.1007/s00249-011-0734-z.

Oral presentation:

1) **Doan-Xuan, Q. M.**, Sarvari, A. K., Fischer-Posovszky, P., Wabitsch, M., Balajthy, Z., Fesus, L. and Bacso, Z. Seeing the cell face, knowing the cell fate. 7th Molecular Cell and Immune Biology Winter Symposium, Galyatető, Hungary, January 7-10, 2014.
2) **Doan-Xuan, Q. M.**, Szalóki, N., Tóth, K., Szöllősi, J., Bacso, Z. and Vámosi, G. Proteins' interaction: don't fret, FRET it. 6th Molecular Cell and Immune Biology Winter Symposium, Galyatető, Hungary, January 8-11, 2013.
3) Nagy, G., **Doan-Xuan, Q. M.**, Gáspár, K., Mócsai, G., Kapitány, A., Törőcsik, D., Bacso, Z., Gyimesi, E., Remenyik, É., Bíró, T. and Szegedi, A. Immunophenotyping by imaging cytometry in atopic dermatitis. 5th Molecular Cell and Immune Biology Winter Symposium, Galyatető, Hungary, 4-7 January, 2012.
4) **Doan-Xuan, Q. M.**, Bacso, Z. Relationship between DNA damage and Annexin V positivity in different apoptosis inductions determined by laser scanning imaging cytometry. Tudományos Diákköri Konferencia, University of Debrecen, April 2-4, 2008.
5) **Doan-Xuan, Q. M.**, Szalóki, N., Tóth, K., Szöllősi, J., Bacso, Z. and Vámosi, G. Fluorescence resonance energy transfer analysis of interaction of cellular proteins using slide based triple-laser cytometry. Tudományos Diákköri Konferencia, University of Debrecen, February 19-23, 2007.
6) **Doan-Xuan, Q. M.**, Bacso, Z. Quantitative detection of large DNA fragments by using pulsed-field gel electrophoresis alkaline comet assay and slide-based imaging cytometer. Tudományos Diákköri Konferencia, University of Debrecen, April 10-14, 2006.

Posters:

1) **Doan-Xuan, Q. M.**, Sarvari, A. K., Fischer-Posovszky, P., Wabitsch, M., Balajthy, Z., Fesus, L. and Bacso, Z. High content analysis of differentiation and cell death in human adipocytes. 18th Leipziger Workshop, Cytomics and Congenital Heart Disease, Leipzig, Germany, April 17-19, 2013.
2) Nagy, G., **Doan-Xuan, Q.-M.**, Gáspár, K., Mócsai, G., Kapitány, A., Törőcsik, D., Bacsó, Z., Gyimesi, E., Remenyik, É., Bíró, T. and Szegedi, A. The role of myeloid dendritic cells in the Polarization of effector T cells in atopic dermatitis. 42nd Membrán-Transzport Konferencia, Sümeg, Hungary, May 15-18, 2012.
3) **Doan-Xuan, Q.-M.**, Szalóki, N., Tóth, K., Szöllősi, J., Bacso, Z. and Vámosi, G. Förster resonance energy transfer analysis of nuclear proteins by laser scanning cytometry. 8th European Biophysics Congress (EBSA), Budapest, Hungary, August 23-27, 2011.